On-Surface Synthesis

International Edition: DOI: 10.1002/anie.201600684
German Edition: DOI: 10.1002/ange.201600684

Post-Synthetic Decoupling of On-Surface-Synthesized Covalent Nanostructures from Ag(111)

*Atena Rastgoo-Lahrood, Jonas Björk, Matthias Lischka, Johanna Eichhorn, Stephan Kloft, Massimo Fritton, Thomas Strunskus, Debabrata Samanta, Michael Schmittel, Wolfgang M. Heckl, and Markus Lackinger**

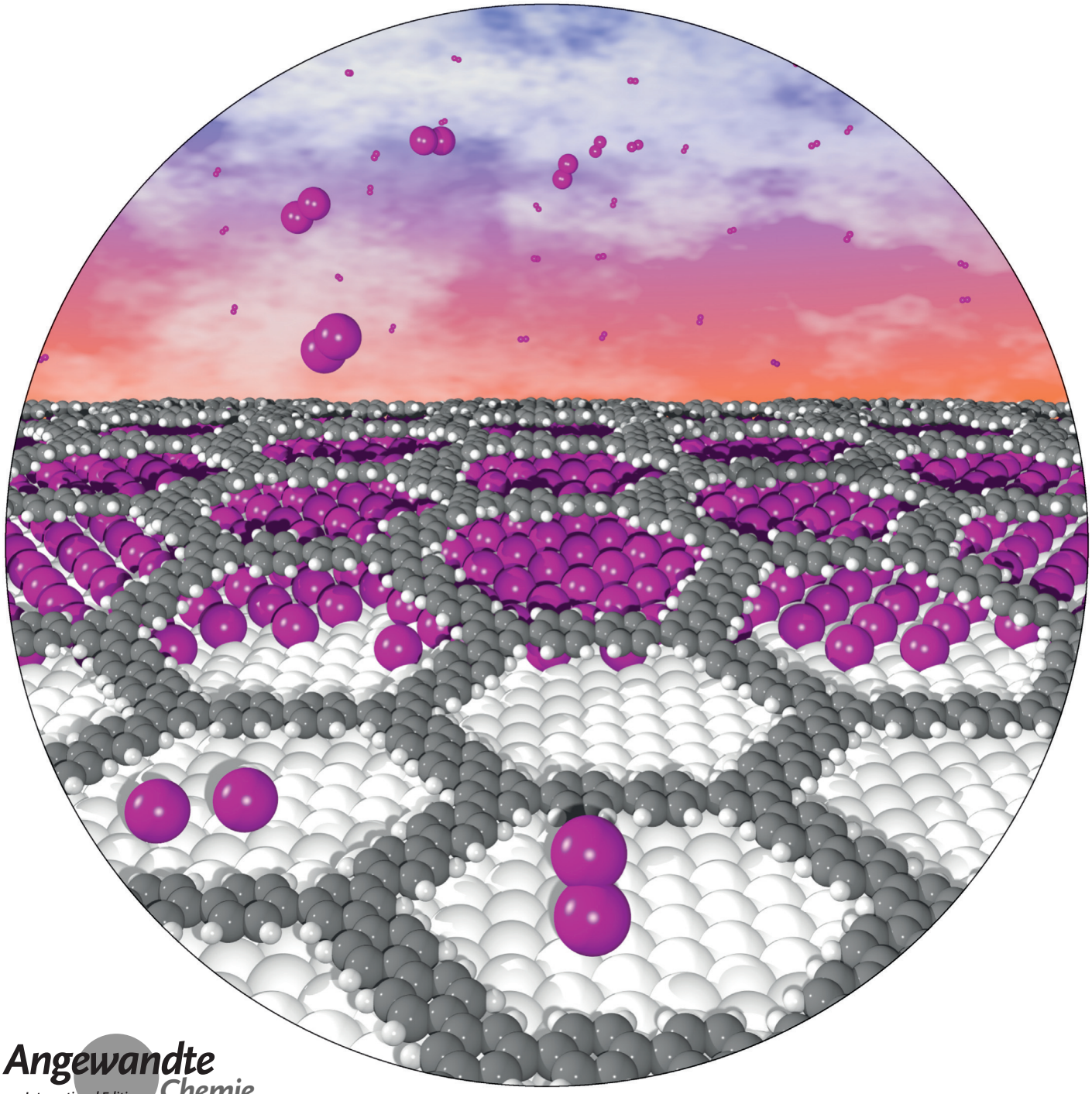

Abstract: *The on-surface synthesis of covalent organic nanosheets driven by reactive metal surfaces leads to strongly adsorbed organic nanostructures, which conceals their intrinsic properties. Hence, reducing the electronic coupling between the organic networks and commonly used metal surfaces is an important step towards characterization of the true material. We demonstrate that post-synthetic exposure to iodine vapor leads to the intercalation of an iodine monolayer between covalent polyphenylene networks and Ag(111) surfaces. The experimentally observed changes from surface-bound to detached nanosheets are reproduced by DFT simulations. These findings suggest that the intercalation of iodine provides a material that shows geometric and electronic properties substantially closer to those of the freestanding network.*

The synthesis of extended 1D and 2D organic nanostructures by direct covalent coupling of monomers on solid surfaces is a rapidly advancing field.[1] Diverse coupling strategies have successfully been employed for the on-surface synthesis of unique covalent organic nanosheets that are inaccessible by other synthetic means.[2] With a view to potential applications, the extraordinary mechanical, thermal, and chemical stabilities of covalent networks offer crucial advantages over self-assembled supramolecular structures. Moreover, the prospect of electrical conductivity renders these materials particularly promising for molecular electronics.[3] However, many important coupling reactions proceed on reactive metal surfaces. On-surface Ullmann coupling, for example, is in most cases initiated on metals by a surface-supported dissociation of the carbon–halogen bond.[4] The approach has also been demonstrated on graphene and hexagonal boron nitride on Ni(111), but the restricted diffusion of the dehalogenated species only facilitated growth of smaller oligomers.[5] In principle, thermally activated Ullmann coupling is also feasible on insulator surfaces, but requires appropriate anchoring to prevent desorption.[6] Nevertheless, metal surfaces bear many advantages, but for many, and in particular for electronic applications, conducting supports are precluded. In cases where coupling does not proceed on inert surfaces, post-synthetic transfer, as routinely applied for graphene grown by chemical vapor deposition (CVD),[7] is a conceivable alternative. Even though the proof of principle has been demonstrated for bottom-up-fabricated covalent nanostructures, for example, by template stripping,[8] transfer remains challenging.

Ullmann coupling under conditions with iodine excess—both under ambient conditions and ultrahigh vacuum (UHV)—provided evidence for the detachment of smaller covalent nanostructures from the metal surface after their formation and subsequent adsorption on top of a closed iodine monolayer (Scheme 1).[9] The affinity of iodine to metals is apparently strong enough to overcome interactions between the surface and organic nanostructures. Motivated by these observations, the present study aims to explore the deliberate exposure of metal-adsorbed covalent nanostructures to iodine vapor as a novel and straightforward approach for post-synthetic decoupling. In earlier studies, post-dosing with bismuth was shown to weaken adsorbate–surface interactions.[10] However, bismuth first coadsorbs on uncovered areas of the surface, and then grows into multilayers for higher coverages, whereas the goal of the present study is the detachment of more extended covalent organic networks through intercalation of a nonmetallic monolayer. All preparation steps were carried out under UHV. Samples were characterized in situ before and after iodine exposure by scanning tunneling microscopy (STM), X-ray photoelectron spectroscopy (XPS), and near-edge X-ray absorption fine structure (NEXAFS) spectroscopy. Alterations in the geometric and electronic structures were studied by density functional theory (DFT) calculations (see the Supporting Information for experimental and computational details).

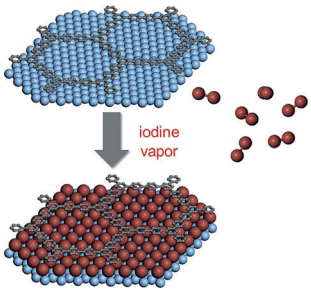

Scheme 1. Basic principle of the post-synthetic decoupling of covalent networks from metal surfaces by deliberate exposure to iodine vapor.

Two-dimensional porous covalent polyphenylene networks derived from 1,3-bis(*p*-bromophenyl)-5-(*p*-iodophenyl)benzene precursors (BIB, see inset in Figure 2c for structure) on Ag(111) were chosen as the model system.[11] In a first step, covalent networks were prepared by deposition of BIB onto Ag(111) at room temperature followed by annealing at about 270 °C. In the next step, samples were exposed to I_2 vapor (5×10^{-7} mbar, ca. 5 min). XPS measure-

[*] A. Rastgoo-Lahrood, M. Lischka, Dr. J. Eichhorn, S. Kloft, M. Fritton, Prof. Dr. W. M. Heckl, Prof. Dr. M. Lackinger
Department of Physics, Technische Universität München
James-Franck-Strasse 1, 85748 Garching (Germany)
and
Deutsches Museum
Museumsinsel 1, 80538 München (Germany)
and
Nanosystems-Initiative-Munich and Center for Nanoscience
Schellingstrasse 4, 80799 München (Germany)
E-mail: markus@lackinger.org
Dr. J. Björk
Department of Physics, Chemistry and Biology
IFM Linköping University
58183 Linköping (Sweden)
Dr. T. Strunskus
Institute for Materials Science—Multicomponent Materials
Christian-Albrechts-Universität zu Kiel
Kaiserstrasse 2, 24143 Kiel (Germany)
Dr. D. Samanta, Prof. Dr. M. Schmittel
Center of Micro- & Nanochemistry & Engineering
Organische Chemie I, Universität Siegen
Adolf-Reichwein-Strasse 2, 57068 Siegen (Germany)

Supporting information for this article can be found under: http://dx.doi.org/10.1002/anie.201600684.

ments conducted before and after iodination are depicted in Figure 1. The I3d spectrum shows a marked increase in surface-bound iodine after exposure, whereas the C1s spectrum indicates a constant amount of carbon. The measured $I3d_{5/2}$ binding energy of 619.0 eV agrees with references for chemisorbed atomic iodine,[12] thus confirming dissociative adsorption of I_2. The C1s peak on bare Ag(111) is slightly asymmetric with a small shoulder at higher binding energies, whereas this feature disappears after exposure to iodine and the C1s peak becomes symmetric. This spectroscopic signature originates from direct interactions with the free electron gas of the metal. Hence, its disappearance indicates both detachment and decoupling upon iodination (see the Supporting Information).

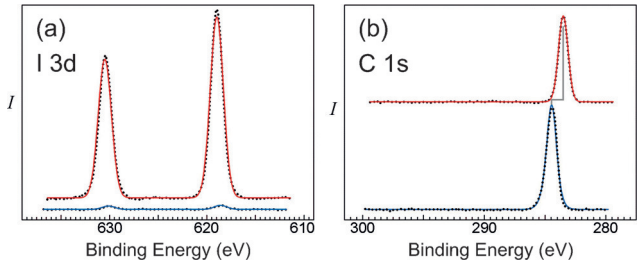

Figure 1. a) I3d and b) C1s XP spectra acquired before (lower spectra, blue lines) and after (upper spectra, red lines) exposure to iodine (offset for clarity). I3d consists of a 3/2 and 5/2 spin-orbit doublet. The small amount of pre-adsorbed iodine originates from the deiodination of BIB preceding formation of the covalent network. C1s exhibits a shift of about 0.92 eV to lower binding energies after iodination, while the line shape changes from slightly asymmetric to symmetric.

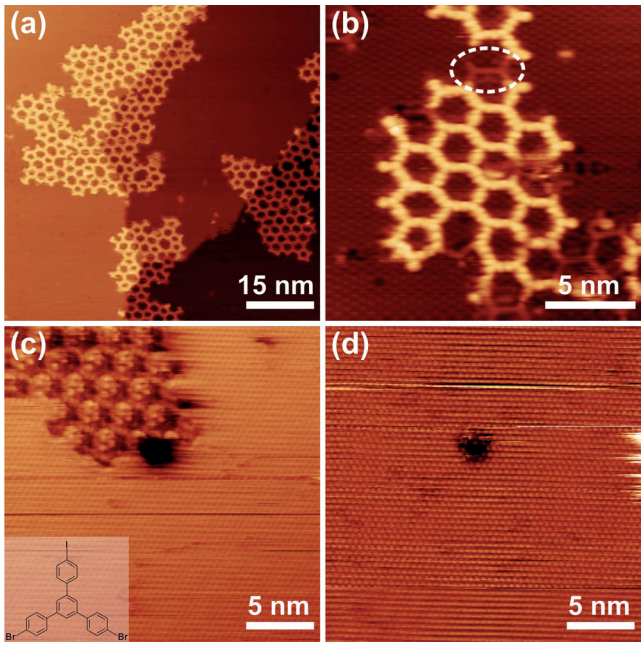

Figure 2. STM images acquired after exposure to iodine. a) Overview ($U_T = -516$ mV, $I_T = 20$ pA) and b) close-up ($U_T = +800$ mV, $I_T = 20$ pA). The dashed oval marks an occasionally observed contrast variation within the network. Lateral manipulation of a covalent network revealed a close-packed iodine monolayer underneath. STM images of the same sample area c) before ($U_T = +500$ mV, $I_T = 30$ pA) and d) after ($U_T = -500$ mV, $I_T = 30$ pA) the network was removed. The dark area is an iodine vacancy island and serves as a site marker. Inset in (c): chemical structure of BIB.

The initial structural characterization was carried out by STM. The overview image in Figure 2a depicts covalent networks that grow over step edges, but otherwise appear higher (brighter) than the respective terraces, while the close-up image in Figure 2b reveals a new hexagonal structure with a lattice parameter of (0.50 ± 0.03) nm, which corresponds to the known $\sqrt{3} \times \sqrt{3}$ R30° iodine superstructure on Ag(111).[12] In accordance with XPS, this new structure is identified as a densely packed iodine monolayer. Another iodine superstructure was occasionally observed (see the Supporting Information). The STM data clearly confirm the adsorption of iodine, but cannot settle the central question: Does iodine only coadsorb on the free surface areas or does it detach the covalent networks and form a closed monolayer underneath? This crucial point was addressed by lateral manipulation of a covalent domain, which revealed a close-packed iodine monolayer underneath. The corresponding STM images are shown in Figure 2c,d. Rapid refilling of the large void space, which would be created directly after displacement of the covalent network, by surface diffusion of iodine from the metal can be excluded: even monoatomic iodine vacancies remain immobile for more than five minutes at the imaging temperature of about 80 K (see the Supporting Information).

Moreover, a pronounced variation in the height and contrast was observed occasionally within the covalent networks; an example is marked in Figure 2b. Integral parts of the network appear lower, thus indicating adsorption directly on the metal surface. Conversely, this implies that the majority of the polyphenylene network is indeed detached from the Ag(111) surface. In addition, the part of the network on the iodine layer not only appears higher, but also exhibits internal contrast, which is unprecedented for networks directly absorbed on metals. This STM contrast resembles the HOMO of the free-standing network (see the Supporting Information), thereby providing further experimental evidence for substantial weakening of the coupling.[13]

Additional structural characterization was carried out by NEXAFS.[14] The samples were again measured before and after exposure to iodine. The normalized C1s NEXAFS spectra are summarized in Figure 3. The most evident changes are increased intensities at larger X-ray incidence angles (e.g. 90°) and decreased intensities at smaller incidence angles (e.g. 30°) after exposure, thus already indicating a change in the adsorption geometry towards increased tilt angles of the phenyl groups with respect to the surface plane. From a more detailed analysis of the dependence of the intensities on the incidence angle, tilt angles of (15 ± 5)° and (35 ± 5)° for the phenyl groups were extracted before and after iodination, respectively (see the Supporting Information). This pronounced change can be explained consistently by intercalation of an iodine monolayer: According to DFT simulations, the phenyl groups in a freestanding polyphenylene network would feature relatively large tilt angles of about 23° as

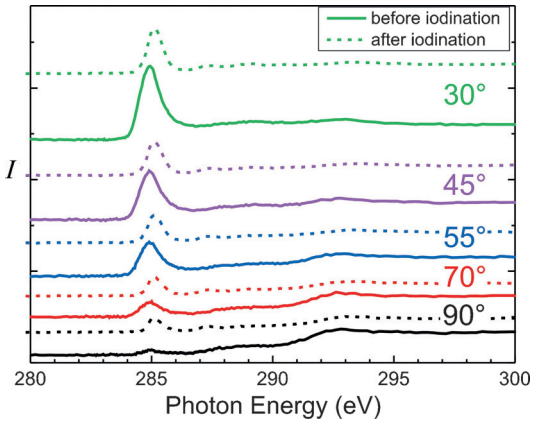

Figure 3. NEXAFS spectra acquired for various incidence angles before (solid lines) and after (dashed lines) exposure to iodine (offset for clarity). Note that the incidence angle is defined with respect to the surface plane, that is, 90° corresponds to normal incidence. The prominent resonance at a photon energy of about 285 eV arises from a C1s→π* transition.

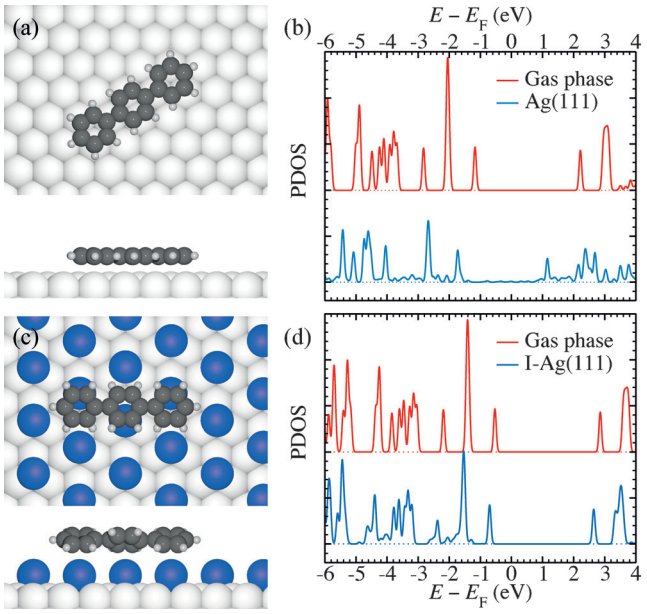

Figure 4. DFT-optimized adsorption geometries and corresponding PDOS of carbon atoms for *p*-terphenyl on: a,b) pristine and c,d) iodine-terminated Ag(111). The upper and lower parts of (a) and (c) show the top and side views, respectively. The PDOS were evaluated for the optimized equilibrium positions (lower spectra in (b) and (d), blue and violet lines) as well as in the gas phase (upper plots, red lines), with the vacuum level aligned to those of the surface systems.

a result of steric hindrance of the *ortho*-hydrogen atoms (see the Supporting Information). Upon adsorption on a metal, this steric hindrance is partly overcome by attractive molecule–surface interactions, thereby resulting in smaller tilt angles. Interestingly, these interactions are not strong enough on Ag(111) to enforce a fully planar adsorption. After intercalation of an iodine monolayer, molecule–surface interactions become significantly weaker than on the bare metal surface. This facilitates relaxation toward the structure of a freestanding network, that is, larger tilt angles of the phenyl groups.

Complementary DFT calculations were conducted on bare and iodine-terminated Ag(111) to substantiate the hypothesis that larger tilt angles indicate polyphenylene networks on top of a closed iodine monolayer. *p*-Terphenyl was chosen as a reasonably sized model system as its phenyl–phenyl σ bonds represent the main structural feature of the actual polyphenylene network. Optimized structures for the lowest energy adsorption sites are depicted in Figure 4 (see the Supporting Information for additional results). The DFT-optimized structure of *p*-terphenyl on bare Ag(111) shows planar adsorption, whereas on iodine-terminated Ag(111) it exhibits a tilt angle, that is, half of the phenyl–phenyl dihedral angle, of 19°. However, an adsorption geometry with a tilt angle of 9.5° was found to be energetically equal to fully planar adsorption on bare Ag(111). In any case, DFT and NEXAFS agree insofar as the tilt angles of phenyl groups on iodine-terminated Ag(111) are larger than on pristine Ag(111), hence providing further evidence for the intercalation of iodine. In addition, DFT results in a substantial reduction of the adsorption energy from −1.49 eV on pristine Ag(111) down to −0.84 eV on iodine-terminated Ag(111). Moreover, DFT provides complementary evidence for electronic decoupling of the organic networks from the metal surface by the iodine monolayer. Figure 4b,d shows the partial density of electronic states (PDOS) projected onto the carbon atoms of *p*-terphenyl on both surfaces compared to in the gas phase. The PDOS changes significantly upon adsorption on bare Ag(111), whereas changes on iodine-terminated Ag(111) are minor, hardly affecting the frontier molecular orbitals. Further experimental evidence for a significantly weakened electronic coupling between the polyphenylene networks and Ag(111) after exposure to iodine comes from NEXAFS. For an incidence angle of 45° the full-width at half-maximum (FWHM) of the C1s→π* resonance is reduced from 0.99 eV on Ag(111) down to 0.73 eV after iodine intercalation (see the Supporting Information). Similar effects are well known for monolayers versus multilayers,[15] and indicate significantly weaker coupling to the surface.

In summary, we propose iodine intercalation as a novel, straightforward, and widely applicable approach for the post-synthetic decoupling of on-surface-synthesized covalent organic nanostructures from Ag(111). Through a combination of STM, XPS, and NEXAFS, it was demonstrated that exposure of covalent polyphenylene networks adsorbed on Ag(111) to iodine vapor results in their detachment from the metal surface through intercalation of an iodine monolayer. NEXAFS and DFT consistently find a structural relaxation as the tilt angles of the phenyl groups increased after iodine intercalation, thereby indicating a weakened molecule–surface interaction for the iodine monolayer compared to the bare metal. This is consistent with the markedly reduced adsorption strength on iodine-terminated surfaces found from DFT calculations. In addition, DFT simulations suggest a significant weakening of the electronic coupling to the metal surface through the presence of a single monolayer of iodine. Experimental evidence is provided both by the change in the line shape by XPS as well as sharpening of the C1s→π*

resonance by NEXAFS after exposure to iodine. Charge transfer, hybridization, and surface polarization affect the electronic structure of molecular networks directly adsorbed on metals.[16] Since these effects are not easily taken into account by simulations, decoupling by the intercalation of iodine facilitates more meaningful comparisons, for example, of electronic band gaps, between theory and experiment. In particular, our approach allows the characterization of intrinsic electronic properties of covalent nanostructures. We also anticipate advantages for transfer by stamping, as the reduced adsorption strength promotes detachment.

Acknowledgements

Financial support by the DFG (LA1842/4-1) and Nanosystems Initiative Munich is gratefully acknowledged. We thank the Helmholtz-Zentrum Berlin for allocation of synchrotron radiation beamtime and financial support. Computational resources were allocated at the National Supercomputer Centre, Sweden.

Keywords: covalent networks · decoupling · surface chemistry · scanning probe microscopy · X-ray absorption spectroscopy

How to cite: *Angew. Chem. Int. Ed.* **2016**, *55*, 7650–7654
Angew. Chem. **2016**, *128*, 7650–7784

[1] a) A. Gourdon, *Angew. Chem. Int. Ed.* **2008**, *47*, 6950–6953; *Angew. Chem.* **2008**, *120*, 7056–7059; b) M. Lackinger, W. M. Heckl, *J. Phys. D* **2011**, *44*, 464011; c) R. Lindner, A. Kühnle, *ChemPhysChem* **2015**, *16*, 1582–1592; d) F. Klappenberger, Y. Q. Zhang, J. Björk, S. Klyatskaya, M. Ruben, J. V. Barth, *Acc. Chem. Res.* **2015**, *48*, 2140–2150; e) Q. T. Fan, J. M. Gottfried, J. F. Zhu, *Acc. Chem. Res.* **2015**, *48*, 2484–2494.

[2] a) J. M. Cai, P. Ruffieux, R. Jaafar, M. Bieri, T. Braun, S. Blankenburg, M. Muoth, A. P. Seitsonen, M. Saleh, X. L. Feng, K. Müllen, R. Fasel, *Nature* **2010**, *466*, 470–473; b) J. A. Lipton-Duffin, J. A. Miwa, M. Kondratenko, F. Cicoira, B. G. Sumpter, V. Meunier, D. F. Perepichka, F. Rosei, *Proc. Natl. Acad. Sci. USA* **2010**, *107*, 11200–11204.

[3] D. F. Perepichka, F. Rosei, *Science* **2009**, *323*, 216–217.

[4] a) J. Björk, F. Hanke, S. Stafstrom, *J. Am. Chem. Soc.* **2013**, *135*, 5768–5775; b) R. Gutzler, H. Walch, G. Eder, S. Kloft, W. M. Heckl, M. Lackinger, *Chem. Commun.* **2009**, 4456–4458.

[5] C. Morchutt, J. Björk, S. Krotzky, R. Gutzler, K. Kern, *Chem. Commun.* **2015**, *51*, 2440–2443.

[6] M. Kittelmann, P. Rahe, M. Nimmrich, C. M. Hauke, A. Gourdon, A. Kühnle, *ACS Nano* **2011**, *5*, 8420–8425.

[7] C. Mattevi, H. Kim, M. Chhowalla, *J. Mater. Chem.* **2011**, *21*, 3324–3334.

[8] M. B. Wieland, A. G. Slater, B. Mangham, N. R. Champness, P. H. Beton, *Beilstein J. Nanotechnol.* **2014**, *5*, 394–401.

[9] a) G. Eder, E. F. Smith, I. Cebula, W. M. Heckl, P. H. Beton, M. Lackinger, *ACS Nano* **2013**, *7*, 3014–3021; b) A. Rastgoo Lahrood, J. Björk, W. M. Heckl, M. Lackinger, *Chem. Commun.* **2015**, *51*, 13301–13304.

[10] N. A. Frei, C. T. Campbell, *J. Phys. Chem.* **1996**, *100*, 8402–8407.

[11] J. Eichhorn, T. Strunskus, A. Rastgoo-Lahrood, D. Samanta, M. Schmittel, M. Lackinger, *Chem. Commun.* **2014**, *50*, 7680–7682.

[12] J. Bushell, A. F. Carley, M. Coughlin, P. R. Davies, D. Edwards, D. J. Morgan, M. Parsons, *J. Phys. Chem. B* **2005**, *109*, 9556–9566.

[13] J. Repp, G. Meyer, S. M. Stojkovic, A. Gourdon, C. Joachim, *Phys. Rev. Lett.* **2005**, *94*, 026803.

[14] G. Hähner, *Chem. Soc. Rev.* **2006**, *35*, 1244–1255.

[15] a) D. Käfer, G. Witte, *Chem. Phys. Lett.* **2007**, *442*, 376–383; b) Y. Zou, L. Kilian, A. Schöll, T. Schmidt, R. Fink, E. Umbach, *Surf. Sci.* **2006**, *600*, 1240–1251.

[16] P. Ruffieux, J. M. Cai, N. C. Plumb, L. Patthey, D. Prezzi, A. Ferretti, E. Molinari, X. L. Feng, K. Müllen, C. A. Pignedoli, R. Fasel, *ACS Nano* **2012**, *6*, 6930–6935.

Received: January 21, 2016
Revised: February 27, 2016
Published online: April 29, 2016

